Numerical Modelings of the Climatic Effects of the Land–Sea Distribution and Topography①

Qian Yongfu (钱永甫)
Department of Atmospheric Sciences, Nanjing University, Nanjing 210093

and *Wang Qianqian* (王谦谦)
Nanjing Institute of Meteorology, Nanjing 210044

Received April 3, 1995; revised June 12,1995

ABSTRACT

The effects of the land–sea contrast and the topography on the climatic properties are simulated in this paper by use of a p– σ incorporated coordinate system model in a zonal domain. In this paper we firstly discuss the statistical features of the model and find that the capability of the model is stable, with the same land–sea distribution and topography seven monthly mean climate states are close to one another, their variance is even less than the initial one. Secondly, we focally discuss the effects of the land–sea contrast and the topography on the modeled climate fields. It is pointed out that the land–sea contrast and the topography influence the atmosphere mainly through the heating effect and the former has larger influences on the simulated large scale climate fields than the latter.

Key words: Climate modelings, Land–sea contrast and topography

I. INTRODUCTION

The fundamental cause of the monsoon is the thermal contrast between the land and the sea. Kuo and Qian(1982) have pointed out that the Tibetan Plateau is not the necessary condition for the Asian summer monsoon, however, it does change the intensity of the monsoon and the distribution of precipitation. The authors pointed out recently again that the zonal structures of the summer quasi– stationary circulation systems are basically the same as that of the land–sea contrast and the topography.

It is natural that the effects of topography on the basic climatic features are smaller than that of the land–sea contrast. As it is well known that the basic climate features have the planetary scale both in summer and in winter. Only the land–sea distribution can be corresponding to such a scale. The plateaus and mountains are only the characteristics over the land, their spatial scales are relatively much smaller, therefore, their influences are certainly much smaller, too.It is seen, therefore, that the effects of the plateaus and mountains can be only superposed upon that of the land and consequently strengthen the dynamic and thermal effects of the land. Of course, in the land areas the topographic effects appear again to be very important. Kasahara and Washington (1969), Hahn and Manabe (1975) all pointed out

①Supported by the National Key Project of Fundamental Research "Climate Dynamics and Climate Prediction Theory" and the National Natural Science Foundation of China.

at early time that the Tibetan Plateau plays a very important role in determination both of the position and the intensity of the winter Mongolian High and of the intensity of the summer Indian monsoon and its latitude reached. Plateaus and mountains can also stimulate special weather and climate phenomena in their regions. Kuo and Qian (1981) have pointed out that the Tibetan Plateau intensifies the cumulative convective activities over that area. The authors have simulated the diurnal changes of meteorological fields in the Tibetan Plateau and the Rocky Mountains regions(see Qian and Wang, 1984). They pointed out that the strong diurnal changes are the special phenomenon in the plateau and mountainous areas and have close relationship to the horizontal and vertical scales. Gao et al.(1979) found out that in the Plateau area there is a special phenomenon called "Plateau Monsoon" which has a spatial scale comparable with that of the Plateau.

From above discussions we may conclude that the formation of the basic climatic properties has relationship to the spatial scales of the affecting factors. The land– sea contrast results in the climatic properties with planetary spatial scales, the topography results in the weather and climate features with corresponding spatial scales and at the same time intensifies the contrast between the sea and the land. However, the past studies are rarely concerned with the details of the effects of the land–sea and topography distributions. Most studies discuss the effects of the topography by comparisons of the experiments with and without mountains and scarcely analyze the effects of the land–sea contrast. In this paper we use a zonal domain model system to study the effects of the land–sea contrast and the topography, compare the circulation characteristics at different longitudes and latitudes with different structures of the land–sea contrast and the topography, and discuss the affecting mechanisms.

II. MODEL SYSTEM AND EXPERIMENTAL SCHEMES

1. *The Model System*

The model system we used in this paper is a land–air and sea– air coupled one. The atmospheric model in the system is a 5–layer primitive equation model with the p–σ incorporated coordinate system in the vertical which adopts the p–system above the 400 hPa level and has 2 layers with the model levels corresponding to the 100 and the 300 hPa levels, respectively. In the atmosphere near the ground surface the σ_b system is used and only 1 layer is there with 50 hPa total thickness. This layer is taken as the atmospheric boundary layer. Between the 400 hPa level and the top of the boundary layer 2 layers with σ system are set. In the atmospheric model, various model physical processes are included and the solar radiation contains diurnal change, as well as the correction due to the changing earth–sun distance(see Qian, 1985).

In the land area there is used a 2 layer soil model. The first layer represents the diurnal changes of the soil temperatures and moistures, while the second layer the annual changes. The layer thickness is determined according to the physical properties of the 5 type underlying surfaces. The details of the soil model can be found in Qian's papers (1988, 1991). The types of the underlying surfaces have been given in Qian's another paper (1993a). The surface albedos depend on not only the soil types but also the soil moisture and the orographic height.

In the ocean there is a 2 layer oceanic model, the first of which has a 50 m thickness and represents the oceanic mixing layer, the second layer is of 250 m and represents the thermoclinic layer, there is no oceanic current in the model (see Qian, 1993b).

2. *Experimental Schemes*

Two groups of experiments are made. The first one is conducted in order to test the statistical capabilities of the model system and designated by MTEX. The second one is specially designed for studying the effects of the land–sea contrast and the topography on the climatic features and designated by LSEX.

In the MTEX there are altogether 7 experiments, each one takes different initial fields but with very small differences and is time integrated up to 30 days. The solar declination is fixed on July 15, therefore, the mean fields of every hour results of the 30 days can be considered as the representative climatic mean fields of July, and there are 7 such monthly means. From the 7 monthly means a July mean climate state can be obtained again. Investigation of the variance of the 7 monthly mean fields from the July mean climate state can get the statistical capability of the model system and this is also a model testing scheme. In order to exclude the effects of other factors on the results the seasonal and diurnal changes are not included in the time integrations, only one type of underlying surfaces that is the clay pasture is used in the land area, but the land–sea contrast and the topography are contained in all the experiments.

In the LSEX, besides the land–sea contrast and the topography, different types of underlying surfaces and the seasonal and diurnal changes are all taken into account. The initial experimental fields are the zonally averaged July geopotential height and moisture fields (see Qian et al.,1994). The initial time is set on June 26, 12:00 GMT. At first the model system is integrated for 5 days to June 30, by this time the zonally averaged initial fields have become zonally nonuniform ones with the coarse properties of summer climate under the effects of the land–sea contrast and the topography. Then another 30 days time integration is further made to get the July mean climate fields by adding every hour results together and dividing the addition by the number of the hours. Discussions on the effects of the land– sea contrast and the topography are conducted based on these mean fields.

III. STATISTICAL TEST OF THE MODEL CAPABILITY

We assume that if the model system can get different monthly mean fields with very small differences started from different initial fields with very small differences, then the model system could be considered stable and the numerical simulations by use of the model system are reliable. Especially when the variance of various monthly mean fields is similar to or even less than that of the various initial fields, the results of the model system are statistically meaningful.

From such a point of view we are going to discuss the model capability. Figs.1a, b, c and Figs. 2a, b, c are root–mean–square error (RMSE) of the 100 hPa level geopotential height, the sea level surface pressure, and the u–components along 90°E of the 7 initial fields and the 7 monthly mean fields, respectively. Form these figures it is seen that in the Tibetan Plateau area the RMSE of the 100 hPa heights, the sea level pressures and the u–components are 30.3 m, 5.31 hPa and 2.3 m / s, respectively, at the initial time, while those corresponding RMSE of the monthly mean fields are 8. 78 m, 1. 2 hPa and 0.5 m / s, respectively. The former values are 4 times larger than the latter values. Over the North and the South American continents such cases can be seen, too. Comparison of Fig. 1 with Fig. 2 also shows that the RMSE of the initial and the monthly mean fields have spatial phase locked features. The maximum RMSEs are always linked to certain geographical areas and the areas with larger RMSE of the initial fields are usually the areas with larger RMSE of the monthly mean fields, and vice

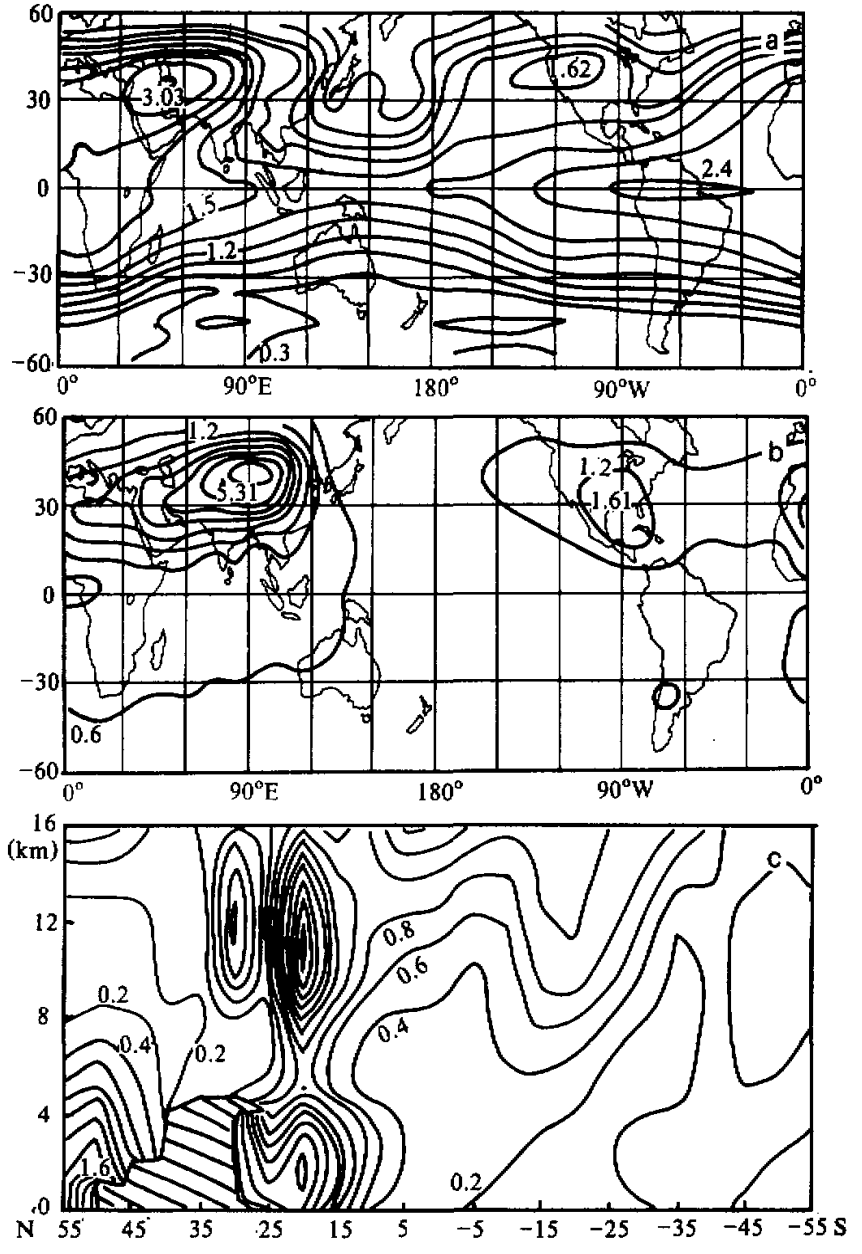

Fig. 1. RMSE of the 7 initial fields in MTEX. a) 100 hPa heights, b) sea level pressures and c) u-components along 90°E.

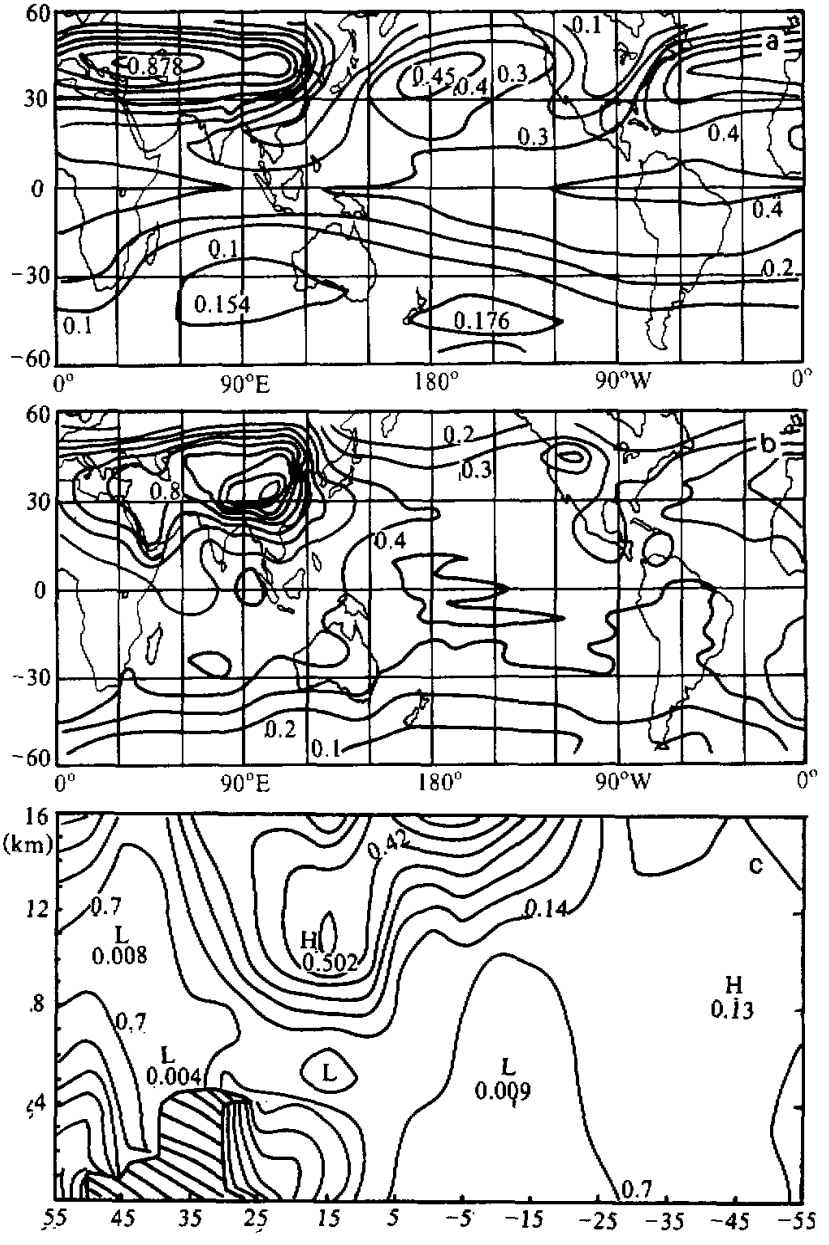

Fig. 2. RMSE of the 7 monthly mean fields in MTEX. a) 100 hPa heights, b) sea level pressures and c) u-components along 90°E.

versa. The larger RMSE of the monthly mean fields may be resulted from the larger RMSE of the initial fields. At the 100hPa level such a distributive property of the RMSE is not as evident as that at the lower levels. The maximum value areas seem to propagate eastward, however, there is always a maximum value area over the Eurasian continent.

Therefore, the capability of the model system we used is stable, under the same land–sea contrast and topography the differences between the initial fields would decrease in the time integration, which makes the monthly mean fields with very small different initial fields close to one another. That means the model system is not sensitive to the initial fields with a little differences. Therefore the numerical experiments made by use of the model system are reliable and meaningful.

IV. DISCUSSIONS OF THE EFFECTS OF THE LAND–SEA CONTRAST AND TOPOGRAPHY ON THE CLIMATIC FEATURES AND THE MECHANISMS

LSEX has the results rather similar to the observed July climatic fields. Here we are not going to give the basic properties of the simulations which can be found in other papers (see Qian et al. , 1994, 1984 and 1993a). The focus of this section is to discuss the effects of the land–sea contrast and the topography, as well as the mechanisms.

In order to discuss the effects of the land–sea contrast and the topography, some representative cross–sections are selected. The first one is a mean profile from 60°E to 120°E (MPR.1), which represents the land–sea and the topography differences between the Tibetan Plateau and its vicinities and the ocean south of the Plateau. The second is also a mean profile from 150°E to 150°W (MPR.2) representing the case of both oceans north and south. The third is from 10°E to 40°E (MPR.3) with both the land areas north and south. A zonal mean meridional profile (ZMPR) is also selected to reflect the total differences between the Northern and the Southern Hemispheres. Those differences are induced by the different seasons and the different topography between the two Hemispheres.

1. *Effects on Temperature Fields*

Fig. 3a is the meridional profile of the zonal mean temperature. It is seen that the simulated meridional distribution of the summer zonal mean temperature is quite close to the observation. At the mid and low latitudes temperature is higher, there is a tropopause at high latitudes of the Southern Hemisphere and the poleward temperature lapse rate is larger than that in the Northern Hemisphere. Fig.3b and 3c are the temperature departures from the zonal mean in MPR.1 and MPR. 2, respectively. Comparison of them with Fig. 3a shows that in MPR.1 there is a positive peak (4.82°C) near 30°N, all departures are positive below 12 km in the Northern Hemisphere and negative above that level. The case is just reversed in MPR.2 where near 30°N there is a negative minimum (−5.59°C), all departures are negative below 12 km and positive above it. The above analysis indicates that the zonal differences of the land–sea distribution and the topography induce the evident differences of the mean temperature distributions between different longitudinal belts. In MPR. 3 the temperature distribution is similar to that in ZMPR as shown in Fig. 3a. This indicates that although in MPR.3 the north–south differences of underlying surfaces are small due to the small heat capacity of the land surface and the different seasons in the Northern and the Southern Hemispheres, and also due to the large land area in the north and the ocean in the south around this section, there still appears the feature of what is warmer in the north and cooler in the south.

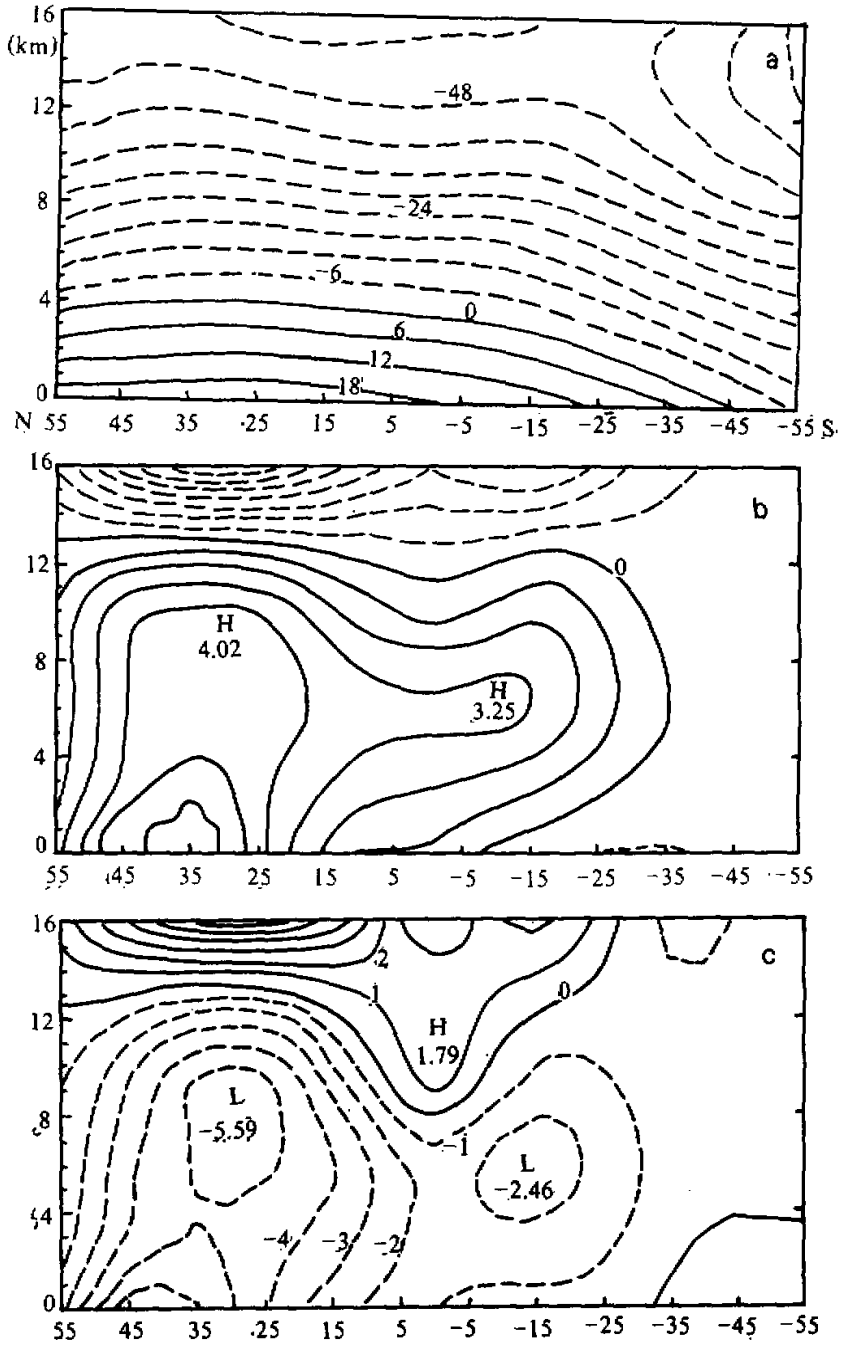

Fig. 3. The meridional profiles of temperatures of LSEX. a) zonal mean in ZMPR, b) mean temperature departures in MPR. 1 and c) mean temperature departures in MPR.2.

2. *Effects on Flow Fields*

Figs.4a and 4b are the u–component distributions in MPR.1 and MPR.2, respectively. The apparent differences can be found between them. In Fig.4a the three wind zones aloft are evident and accompanied with a core of easterly jet. In Fig.4b the three wind zones are still seen although, the easterly jet is weaker and the westerly in the south shifts northward. At low levels the wind belts in Fig.4a are evidently influenced by the topography, there are easterlies north of the Plateau and westerlies in the south, while in Fig.4b the wind systems are simpler with all easterlies at the mid and low latitudes. By comparison of Fig.4a with that in ZMPR (not shown) it is found that they are similar. Therefore, although the areas of the oceans occupy the 70 percent of the globe, the necessary condition which determines the structures of the flow fields is the coexistence of the land and the sea even though the land occupies smaller areas. In MPR.3 the feature as shown in Fig.4a is also seen (omitted) and moreover the picture is closer to that in ZMPR than that shown in Fig. 4a, the cause has already been pointed out.

Figs.4c and 4d are the same profiles as Figs. 4a and 4b but for the v–components. From those figures we can see the evident differences between them. In Fig.4c the low level southerlies start from 40°S, their thickness increases northward, the wind speed exceeds 6 m / s at the equator which reflects strong cross–equatorial air currents there. In Fig.4d the southerlies start from 30°S with maximum speed of only 3 m / s at the equator, there are still some southerly components at the upper troposphere. It is seen, therefore, that the thermal contrast between the Eurasian continent and the oceans south of it, as well as the Tibetan Plateau topography are the main causes to form the strong and widely south to north expanding low level southerly flows.

Figs. 4e and 4f are vertical motions in MPR.1 and MPR.2 (0.1 mm / s). It is seen that in Fig.4e there are all ascent motions in the Northern Hemisphere, the maximum upward motion appears near 5°N at 6km aloft with a value of 1.26 mm / s, the strongest downward motion exists near 10°S at the same height with a value of 1.09 mm / s. In Fig. 4f the ascent motions are greatly reduced and appear only below 8 km. The upward motion near north of the equator is only as large as 0. 214 mm / s, while the descent motion south is still stronger with a value of 1.1 mm / s and extends to 5°N, however, the domain with the stronger descent motions is much smaller than that in Fig.4e. The vertical motions in ZMPR and MPR.3 are similarly distributed as in Fig.4e (omitted). However,in MPR.3 the upward and downward motions on both sides of the equator are stronger and reach 2.3 mm / s and 1.55 mm / s, respectively. Moreover, at 6km aloft near 30°N another downward motion centre appears with a value of 0.25 mm / s, its domain is from 25°N to 43°N through the whole troposphere. This downward motion may have something to do with the desert inside the area and another cause of the downward motion may be the compensative descent motion induced by the upward motion over the Tibetan Plateau east of the area. Therefore, the soil properties of the underlying surfaces and the interactive effects of the flows between the adjacent regions can make the effects of the land– sea contrast and the topography more complicated.

3. *Effects on Vertical Circulations*

The vertical circulations can more evidently show the effects of the land– sea contrast and the topography. Figs.5a,b and c are the mean vertical circulations in MPR.1, MPR.2 and MPR.3, respectively. Due to the evident contrast between the land and the sea in Fig.5a and also the existence of the Tibetan Plateau, there is a very strong meridional circulation between

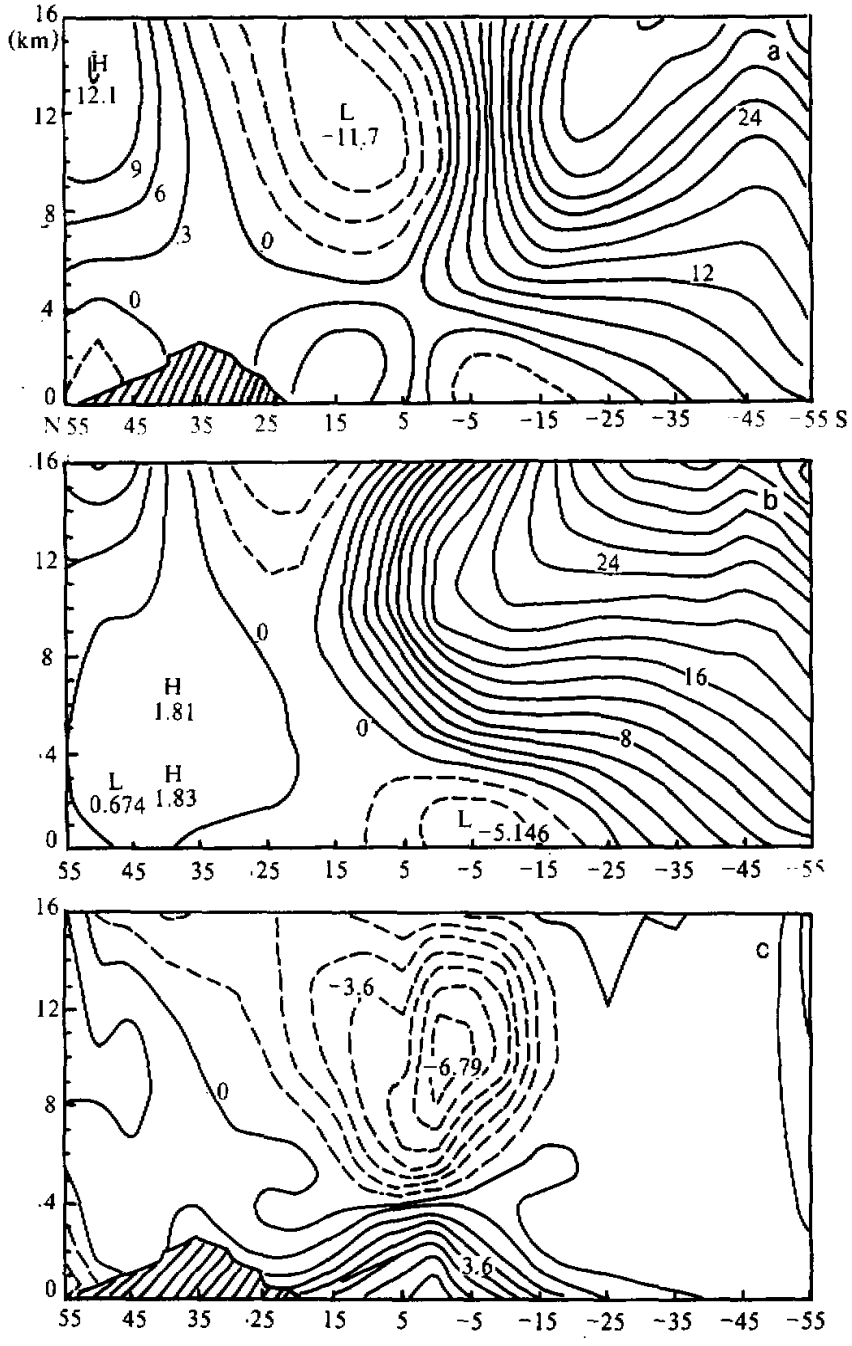
16
(km)
12
8
4
0
H
12.1
L
-11.7
9
6
3
0
0
24
12
a
N 55 45 35 25 15 5 -5 -15 -25 -35 -45 -55 S
b
H
1.81
L
0.674
H
1.83
L
-5.146
24
16
8
0
0
55 45 35 25 15 5 -5 -15 -25 -35 -45 -55
c
-3.6
-6.79
0
3.6
55 45 35 25 15 5 -5 -15 -25 -35 -45 -55

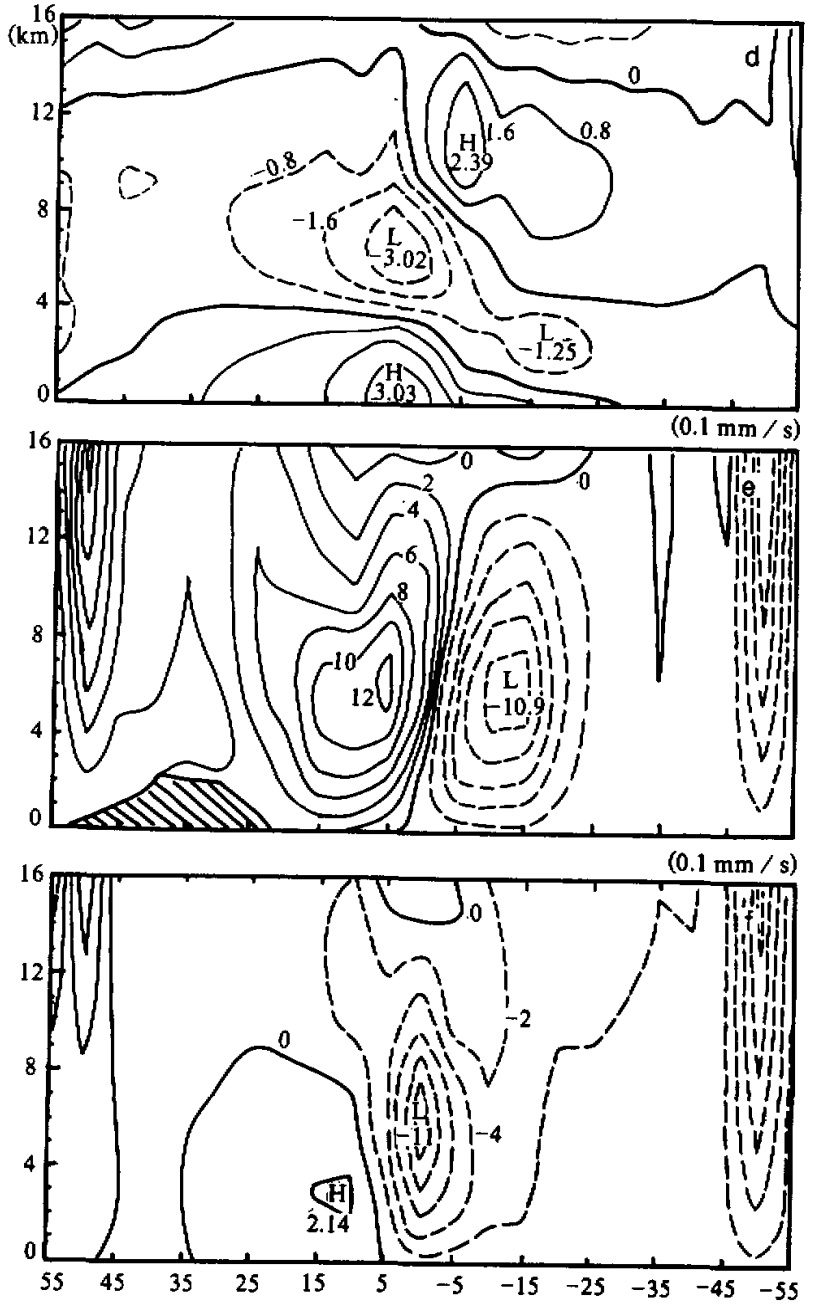

Fig. 4. Distributions of u–components(a,b), the v–components(c,d) and the vertical motions(e,f) in MPR.1(a,c,e) and MPR.2 (b,d,f), respectively, in LSEX. Units: u, v in m / s, w in 0.1 mm / s.

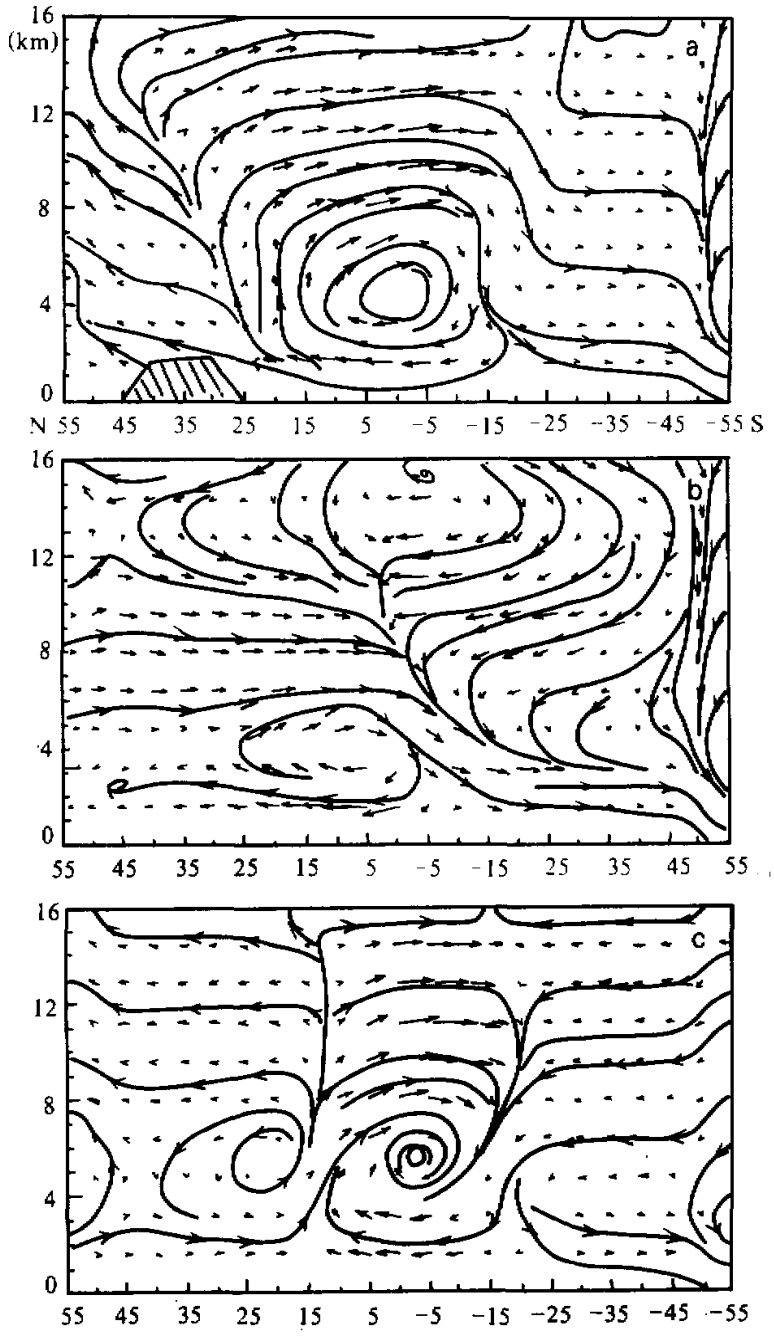

Fig. 5. Mean meridional circulations of LSEX in MPR. 1(a), MPR. 2(b) and MPR. 3(c).

the Northern and the Southern Hemispheres, that is the famous Asian monsoon circulation, it is very similar to that in the zonal mean profile (ZMPR), the only difference is the positions of the upward branches. In Fig. 5b, due to the oceans in both hemispheres, only a small and low level vertical circulation exists between 5°S and 25°N. At the mid and upper troposphere the flow is plain and straight and has obvious convergence. In Fig.5c, due to the complex underlying surfaces, the meridional vertical circulations are more complex, over the equator there is a cell, its upward branch is located in the convergent zone of the low level flow near the equator, its downward branch in the desert region of South Africa. By induction of its downward motion there exists a cell with opposite direction in the mid and high latitudes of the Southern Hemisphere. There is another circulation between the ITCZ of the Northern Hemisphere and the North African desert areas.

Besides the meridional structures there are also zonal structures of the land–sea distributions and the topography which have important influences, too, on the circulation features. We have analyzed the mean circulations in the 10°S–10°N and the 25°N–45°N latitudinal belts and found that they are apparently different (not shown). In the 10°S–10°N belt, the underlying surfaces are basically the ocean, the vertical circulation is simpler and reflects the property of the Walker Cell of the equatorial area. In the 25°N–45°N belt, the distribution of the land and the sea has a zonal two wave structure, and over the land the topography is also complex, therefore, the features of the vertical motions appear as ascending over the land and the coastal areas and descending over the oceans with a zonal two wave structure as well. The upward motions over the Tibetan Plateau and its east side are stronger and broader than that over the North American continent, which fully indicates the influences of the horizontal and vertical spatial scales of topography on the climate features.

4. *Effects on Precipitation Fields*

The precipitation fields have more evident geographic differences. Figs.6a,b,c and d are the meridional distributions of precipitation in ZMPR, MPR.1, MPR.2 and MPR.3, respectively. The capital letters A, B and C show the large scale, the cumulative scale and the total amounts of precipitation, respectively. From Fig.6a it is seen that the precipitation amount in the Northern Hemisphere is more than that in the Southern Hemisphere, the area with large amount of precipitation is located in the ITCZ and the maximum total amount is near 15°N. At the mid and high latitudes of the Northern Hemisphere the cumulative scale precipitation is the main component. The pattern of the precipitation is similar to the observation, but the simulated large scale precipitation in the tropics is more while the cumulative precipitation is less. Comparing Figs. 6b, c and d we can see that the distributions of precipitation are very different in the three meridional belts with different types of land–sea contrast and topography. In the MPR.1 belt with land and the Tibetan Plateau in the north and the oceans in the south, the total and the large scale precipitations have a two–peak structure at low latitudes, from 15°N to 45°N the cumulative precipitation is the main component while the large scale one can almost be neglected, it seems because of the effects of the Tibetan Plateau. In the MPR. 2 belt with oceans both in the south and in the north (Fig. 6c), the main feature is a broad zone of the large scale precipitation and precipitation amount is also relatively much in the Southern Hemisphere. In the meridional belt with land both in the north and in the south (MPR.3, Fig.6d), the precipitation area is very narrow and mainly exists in the convergent zone between 5°S and 25°N, and north of 15°N the cumulative component is the main component of precipitation.

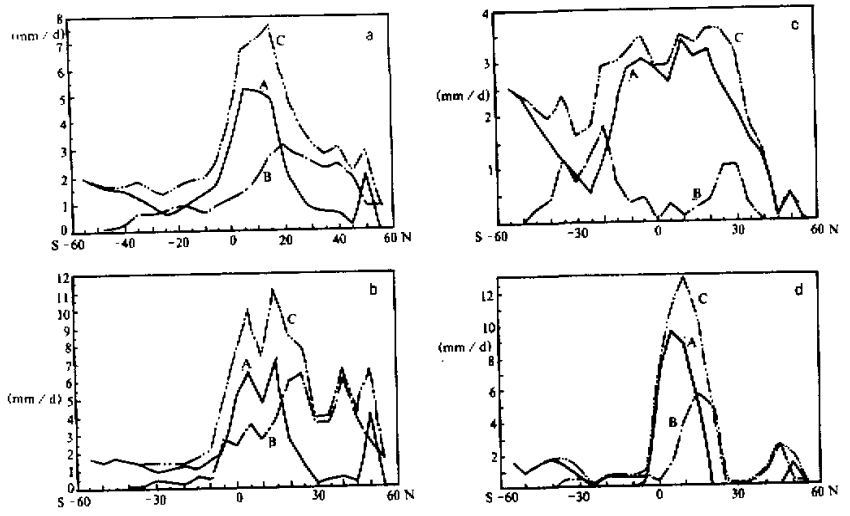

Fig. 6. Meridional distributions of precipitation of LSEX. (a) in ZMPR, (b) in MPR.1, (c) in MPR.2 and (d) in MPR.3. Unit: mm / d. A,B and C indicate the large scale, the cumulative scale and the total amounts of precipitation, respectively.

5. *Effects on Heat Fields and Discussion of Mechanisms*

In order to depict the mechanisms of the effects of the land–sea contrast and the topography on the meteorological fields, in this paragraph the heat fields simulated are analyzed. As we know that the heat fields have three–dimensional structures and to save space we integrated the three–dimensional heat fields in the vertical to get the two–dimensional ones, discussions here are made only for the two–dimensional fields.

From the distributive patterns of the LSEX total heating rates it is seen that the total heating rates are very nonuniform, especially over the land areas with topography (Fig.7a). Over the oceans they are uniform and basically the cooling rates, especially over the North Pacific. In the Northern Hemisphere the feature that the land is the heat source and the ocean the heat sink is very evident, this fully reflects the effects of the land–sea contrast. Over the continental regions the structure of the heat field over the North America is much simpler than that over the Eurasian continent, which just reflects the effects of the topography.

It is seen from the analysis of the contributions of the various heating components to the total heating field that the most important component is the condensation latent heat in the precipitation process. It can be proved by the similarities between the distributions of the total heating field and the precipitation. The longwave radiative heating component and the sensible heat transfer between the land and the air as well as between the ocean and the air also have certain contributions, especially in the case of no condensation, the longwave radiative heating rates are usually the main components.

Figs.7b and 7c are the meridional distributions of the mean heating rates (°C / d) in MPR.1 and MPR.2. The capital letters A,B,C and D denote the total heating rates, the latent heating rates due to condensation, the longwave radiative heating rates and the sensible heating rates due to the heat transfer between the air and the land or the ocean. From Fig. 7b it is seen that the total heating rates are positive in the Northern Hemispheric land areas and

negative over the Southern Hemispheric oceans. The total heating rates are in the range of 1–2°C / d at the most latitudes in the Northern Hemisphere, their distributive pattern is very similar to that of the latent heating rates, but their values are a little smaller than that of the latter because the longwave radiative heating rates are usually negative and their absolute values are larger than that of the sensible heating rates which are usually positive. In Fig. 7c the total heating rates are basically negative especially at high latitudes of the Northern Hemisphere, but the absolute values are all smaller and the extreme values do not exceed 1°C / d. Due to the smallness of both the latent condensation and the sensible heating rates the longwave radiative cooling rates become the main factor determining the total heating rates.

Therefore, the important influences of the land– sea contrast and the topography on the heating fields can be clearly seen by comparison of Fig.7b with Fig.7c. As long as the land–sea difference between the north and the south is larger and there is higher topography over the land the meridional distribution of the heating rates is very nonuniform. To the contrary, when there are oceanic underlying surfaces both in the north and in the south the distribution is more uniform. In summer, the heating effect of the land is obvious while the ocean has cooling effect. It is such a difference in the heating field that induces the differences of meteorological fields. The comparisons of Figs. 5a,b with Figs. 7b,c prove the above point, that is, the heating areas are corresponding to the areas with ascent motions and the cooling areas corresponding to the areas with descent motions. Therefore, the mechanisms of the effects of the land–sea contrast and the topography may be expressed as follows: through the different physical properties of underlying surfaces the land–sea contrast and the topography alter the solar radiation with basically zonal uniformity to the heating factor with nonuniformity in both the latitudinal and the longitudinal directions, which makes the ground surfaces have different temperatures, therefore, the different transfer of the sensible, the latent and the radiative heat between the land and the air or between the ocean and the air takes place, the atmosphere is heated or cooled to different extent. The atmospheric temperatures and the circulation features are correspondently changed and so do the divergence, the convergence and the thermal stability. The condensation process in the atmosphere is also altered to give nonuniform condensation heating which further changes the temperatures and the flow fields in the atmosphere. Such a cycle is continuously going until a certain equilibrium state is reached. Therefore, generally speaking, the heat exchange between the air and the underlying surfaces is not a large term though, it has a trigger effect, this effect is enlarged by the condensation process in the atmosphere and is the fundamental cause of the condensation change. Of course,the nonuniformity of the cloud distribution taking place in the condensation can again induce more nonuniformity of the absorbed solar radiation by the underlying surfaces in the different areas with different land–sea contrast and topography. Therefore, such a process is a feedback process.

V. CONCLUSIONS

After the above analyses and discussions we can see that the model system we used is stable in capability and can be utilized for various numerical experiments.

The land–sea contrast and the topography have very important influences on the climate and circulations. In summer, the Northern Hemispheric land is basically the heating area and the ocean the cooling area. The climatic features of the planetary scale depend on such different thermal effects of the land and the sea. The topography not only intensifies the thermal

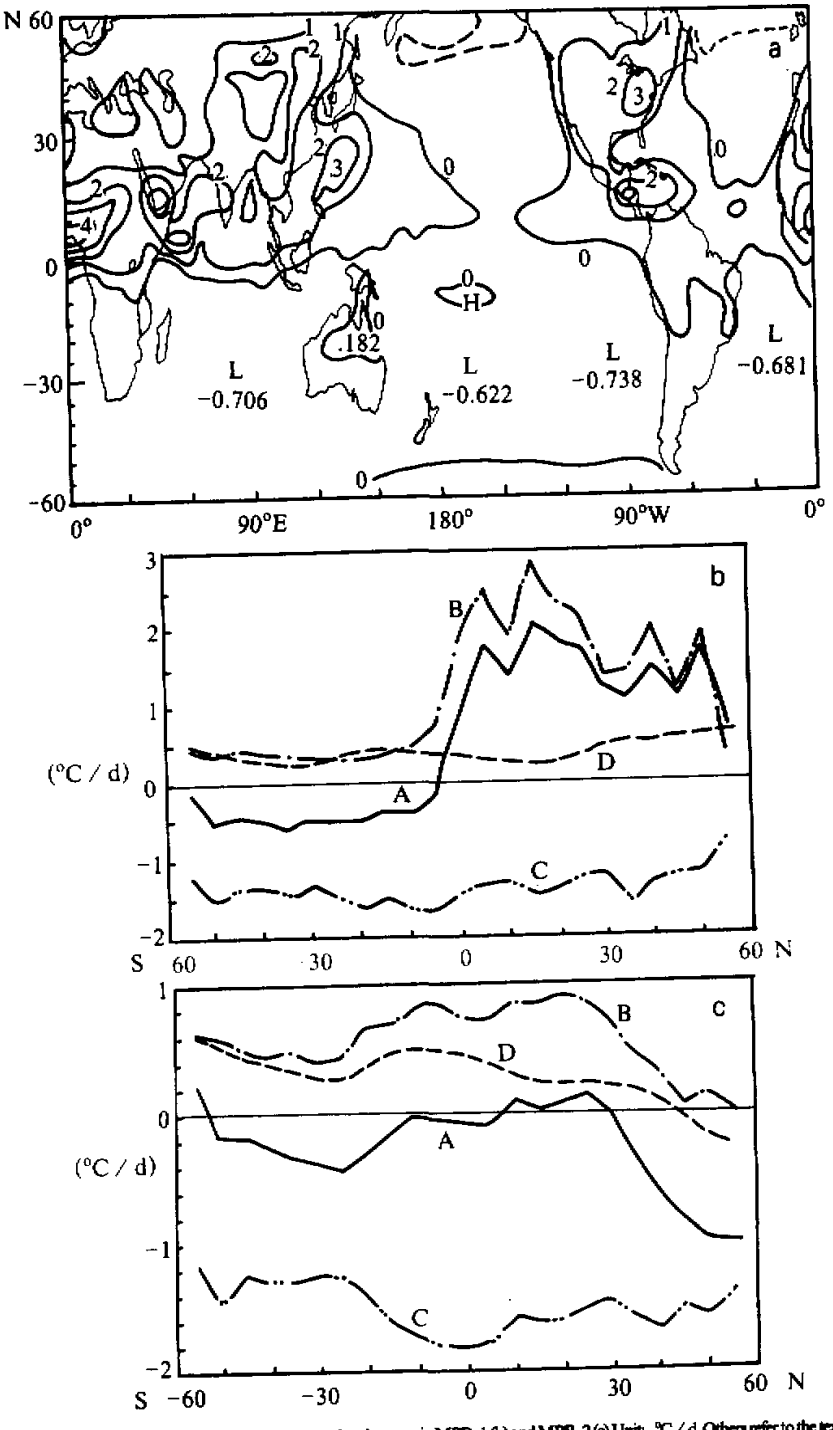

Fig. 7. The LSEX total heating rates (a) the mean heating rates in MPR. 1 (b) and MPR. 2 (c) Unit: °C / d. Others refer to the text.

contrast between the land and the sea, but also influences the circulation features in the orographic areas and makes them more complicated. The affecting scales of the topography depend on the horizontal and the vertical scales of the topography itself. Due to the much smaller scales of the topography than that of the land–sea distributions, the effects of the topography must be the secondary.

From the mechanisms of the effects of the land– sea contrast and the topography it is seen that the thermal effects are the main. Although the exchange amounts of the sensible heat and the radiation between the air and the land or between the air and the ocean are not large,they have trigger effects for changes. The effects on the general circulation mainly come from the condensation process. Therefore, there must be more comprehensive and perfect model physics especially the proper description of the condensation and parameterization schemes to better simulate the climatic features and their changes.

REFERENCES

Hahn, D. and S. Manabe (1975), The role of mountains in the south Asian monsoon circulation, *J. Atmos. Sci.*, **32**: 1515–1541.

Kasahara, A. and W.M. Washington (1969), Thermal and dynamical effects of orography on general circulation of the atmosphere, *Proc. WMO / IUGG Symp. Numerical Weather Prediction in Tokyo*, **IV**: 47–56.

Kuo, H.L. and Y.F. Qian (1981), Influence of the Tibetan Plateau on cumulative and diurnal changes of weather and climate in summer, *Mon. Wea. Rev.*, **109(11)**: 2337–2356.

Kuo, H.L. and Y.F. Qian (1982), Numerical simulation of the development of mean monsoon circulation in July, *Mon. Wea. Rev.*, **110(12)**: 1879–1897.

Qian, Y.F., Y. Qian and Q.Q. Wang (1994), Numerical modelings of the summer quasi–stationary circulation systems and their monthly variations, *Adv. Atmos. Sci.*,**11(4)**: 399–407.

Qian,Y.F. and Q.Q.Wang (1984), A numerical simulation of diurnal variations of meteorological fields in summer, *Adv. Atmos. Sci.*, **1(1)**: 40–52.

Qian, Y.F. (1985), A five–layer primitive equation model with topography, *Plateau Meteorology*, **4(2)(suppl.)**: 1–28.

Qian, Y.F. (1988), A calculation scheme of the ground surface temperature, *Scientia Meteor.Sinica*, **8(4)**: 14–27(in Chinese).

Qian, Y.F. (1991), Numerical simulation of temperature and moisture changes in the coupled land–air system, *Acta Meteor. Sinica*, **49(4)**: 538–547 (in Chinese).

Qian, Y.F. (1993a), Numerical simulations of the effects of underlying surfaces in climate change, *Chinese J. Atmos. Sci.*, **17(2)**: 114–124.

Qian, Y.F. (1993b), Effects of different sea temperatures over the western Pacific on summer monsoon properties, *Acta Oceanologica Sinica*, **12(4)**: 535–547.

Ye, D.Z. and Gao, Y.X. (1979), *The Qinghai–Xizang Plateau Meteorology*, Science Press, Beijing, pp.278 (in Chinese).